

Research Article

Open Access

Giovanni Leucci* and Lara De Giorgi

2D and 3D seismic measurements to evaluate the collapse risk of an important prehistoric cave in soft carbonate rock

Abstract: The southern part of the Apulia region (the Salento peninsula) has been the site of at least fifteen collapse events due to sinkholes in the last twenty years. The majority of these occurred in "soft" carbonate rocks (calcarenes). Man-made and/or natural cavities are sometimes assets of historical and archaeological significance. This paper provides a methodology for the evaluation of sinkhole hazard in "soft" carbonate rocks, combining seismic and mine engineering methods. A case study of a natural cavity which is called Grotta delle Veneri is illustrated. For this example the approach was: i) 2D and 3D seismic methods to study the physical-mechanical characteristics of the rock mass that constitutes the roof of the cave; and ii) scaled span empirical analysis in order to evaluate the instability of the crown pillar's caves.

Keywords: 2D and 3D seismic method; prehistoric cave stability; carbonate rock; safety factor; probability of failure

DOI 10.1515/geo-2015-0006

Received May 29, 2014; accepted June 23, 2014

1 Introduction

The study area is located 40 km south of Lecce, near the Parabita village (Apulia Region, southern Italy; Figure 1). The Parabita area is located on a ridge which is elongated in the NNW-SSE direction, and is locally named Serra di S. Eleuterio. Serra di S. Eleuterio is characterized by limestones and dolomitic limestones with thicknesses ranging from a few centimeters to about 1 m. East of the Serra, more recent sediments outcrop to form a flat surface which

is widely covered by terra rossa deposits. The sediments comprise:

- Calcarenes of Salento, made up of coarse calcarenites from the Lower Pleistocene;
- Subapennine Clays, made up of clayey deposits from the Lower Pleistocene;
- marine terraces of beach and coastal deposits from the Middle–Upper Pleistocene.

Human activities in the area of Parabita are known to have occurred since 80,000 B.C. In fact, in the cave known as Grotta delle Veneri, *Homo Sapiens Neanderthalensis* (Neanderthal) and *Homo Sapiens-Sapiens* (Cro-Magnon) artefacts (35,000 – 10,000 B.C.) were discovered in 1966 [1]. In the same year, two statuettes representing two pregnant women were found (2000 – 10000 B.C.). The Grotta delle Veneri (Cave of the Venus) is one of the most important archaeological sites of the Salento peninsula, and its discovery confirmed the presence of Neanderthal man in the Mediterranean Basin.

Since its discovery, the stability and conservation of Grotta delle Veneri have been a primary concern of local authorities, especially with regard to the stability of the roof. As often happens over the years, the cave has progressively deteriorated and consequently water infiltration has led to an increase in humidity and rock degradation. A number of studies were carried out in order to determine the effects of these environmental alterations within the cave [2]. Current research projects assume that protection of the prehistoric evidence depends mainly on conservation of the cave, which depends on the degree of damage of the cave's roof. The development of these studies, focusing on preventing structural failure of the cave, has a very important application in human heritage protection. UNESCO promotes initiatives for evaluation and conservation of cultural heritage mainly related to restoration or conservation, and only rarely related to prevention of damage [3]. Risk assessment as described at Grotta delle Veneri in this paper, can act as a useful tool in damage prevention. However, as illustrated in [4], karstic areas usually require complex scientific and technical efforts and defin-

*Corresponding Author: Giovanni Leucci: Consiglio Nazionale delle Ricerche – Istituto per i Beni Archeologici e Monumentali, E-mail: g.leucci@ibam.cnr.it

Lara De Giorgi: Consiglio Nazionale delle Ricerche – Istituto per i Beni Archeologici e Monumentali

 © 2015 G. Leucci and L. De Giorgi, licensee De Gruyter Open. This work is licensed under the Creative Commons Attribution-NonCommercial-NoDerivs 3.0 License.



Figure 1: Location of the survey area.

ing unique study methods is very difficult; therefore, it is recommended to determine a strategy that provides flexibility to adjust the specific methods according to local conditions in each region [5].

The stability of karstic caves is being increasingly assessed through the use of geophysical surveys [2, 6–11]. For example, geophysical methods allow a rapid analysis of rock shearing and concrete lining quality [12–15]. In some cases, such methods are a preferred alternative to direct investigation methods that are both costly and difficult to carry out, especially in relatively inaccessible places.

In the present study, a method to evaluate the structural failure risk in prehistoric caves is proposed and applied. The evaluation was performed in four phases: 1) Analysis of the geometry parameters related to the cave; 2) Definition of the physical – mechanical characteristics of the rock that constitute the roof of the cave; 3) Evaluation of the Safety Factor (SF); 4) Determination of failure probability.

The proposed method has been developed using as an example the studies performed in the evaluation of roof failure at abandoned mines. These studies [16] allow the SF to be defined considering empirical relationships that include geometrical parameters such as the constant thickness of ground pillars, the cave's span, and the rock quality parameter defined by the index of [17].

In the present work, the relationships determined by Hutchinson et al. [16] were adapted to karstic caves stability studies. Karstic caves are well known to have a complex geometric shape, and both the thickness of the roof (crown pillars) and its width (span) are variable (Figure 2). These variabilities should be taken into account in stability evaluation.

The physical-mechanical characteristics of the rock were evaluated using 2D seismic travel time tomography and 3D seismic refraction tomography. The structural condi-

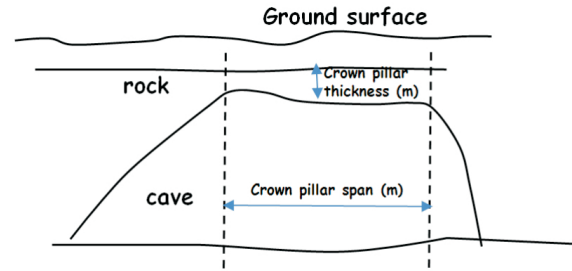


Figure 2: Crown pillar definition scheme.

tion of the Grotta delle Veneri was studied in Leucci and De Giorgi [2] using integrated 2D geophysical methods (Ground-penetrating radar – GPR, and electrical resistivity tomography - ERT). Authors concluded that the integrated geophysical analyses outlined, in the studied area, a highly unstable region.

In this paper, seismic P -wave velocity analysis was used with a revised relationship that accounts for long-term surface stability of the crown pillar. The empirical analysis on the stability of the crown pillar was performed considering the crown pillar's thickness and its span as variables as a function of its length and width respectively.

2 Empirical analysis: the scaled span method

A crown pillar is any rock structure that remains between an underground cave and the ground surface (Figure 2). The thickness of the rock that forms the roof of the cave is defined as the crown pillar thickness. The width of the roof is defined as the crown pillar span.

As described in [16], empirical analysis methods can be used to assess the stability of a crown pillar. The method of assessment is known as the scaled crown pillar span method [18]. This method had been developed from extensive databases containing information about the geometry, rockmass parameters, and stability of crown pillars. The method relies upon two input parameters; one related to the crown pillar geometry, and the other related to the rockmass quality. The rockmass quality is quantified by Q (Tunnelling Quality Index; [19]). Instability of a crown pillar is likely to occur if the scaled crown pillar span, C_s , is greater than the critical span, S_c , calculated from the equation (modified from [18]):

$$S_c = 3.3 \times Q^{0.43} \quad (1)$$

$$C_s = S \sqrt{\frac{SG}{T \left(1 + \frac{S}{L}\right) (1 - 0.4 \cos \theta)}} \quad (2)$$

where S = crown pillar span (m), L = crown pillar length (m), T = crown pillar thickness (m), SG = rockmass specific gravity (= 3.5 for high grade ore; = 3 for moderate grade ore; = 2.7 for waste rock), θ = orebody/foliation dip. The method is applied by comparing the scaled crown pillar span for the pillar of interest to the critical span value deemed appropriate for the controlling rock mass. When the scaled crown pillar span is determined to be less than the critical span, the crown pillar is considered to be stable. On the other hand, when C_s is greater than S_c , the probability of failure is high. Because of its empirical basis, application of the scaled span method allows at least a rational assessment of failure likelihood if the method is applied probabilistically [18]. The index is known as the factor of safety:

$$F = \frac{S_c}{C_s} \quad (3)$$

where instability of a crown pillar is likely to occur if $F < 1$. Table 1 shows how the method can help in defining acceptable or allowable risk.

The empirical relationship between the probability of failure (P_f) and factor of safety (F) was defined by [20]. It is an error function relationship:

$$P_f = 1 - \operatorname{erf} \left[\frac{(2.9F - 1)}{4} \right] \quad (4)$$

As is shown in equation (4), the probability of failure is dependent on both the geometry of the cave and the quality of the rock.

3 Seismic travel time tomography data acquisition and analysis

The position and dimensions of the Grotta delle Veneri were investigated by Leucci [21] using 3D GPR and ERT geophysical methods. Once the thickness of the rock that forms the roof of the cave had been estimated, a seismic traveltime tomography survey was undertaken. The seismic tomography was performed along one line (Figure 3) by distributing 24 geophones and 24 source locations (Figure 4). Twenty-four vertical geophones (14 Hz) with 1 m spacing and 24 shot points (one for each geophone position) were located along two parallel lines. The elastic signal was generated by striking a rod with a hammer. The 24 receivers were placed at the measurement surface

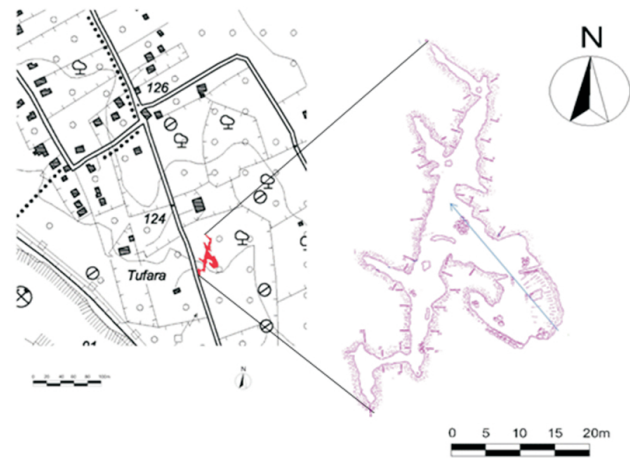


Figure 3: The Grotta delle Veneri study area. The blue arrow highlights the seismic travel time tomography profile location.

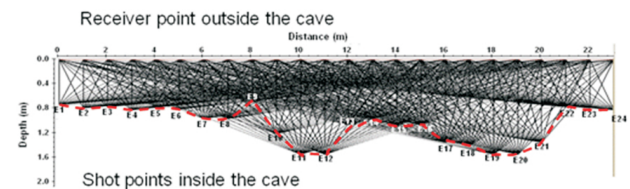


Figure 4: The acquisition geometry of the seismic travel time tomography profile: E denotes the shot positions.

($z = 0$) every 1 m, and 24 shot points (labeled $E1, \dots, E24$ in Figure 4) were placed inside the cave every 1 m corresponding to each receiver's position on the surfaces. This source-receivers geometry (Figure 4) allows to obtain information about the seismic waves velocity in the roof of the cave. The first step in travel time tomography data processing consist in the measurements of the travel times of seismic wave first arrivals related to source - receiver distances. This was done manually (Figure 5a) using reflex software version 6.0 [22]. The travel time analysis was done on the twenty-four seismograms (Figure 5b) and allow to obtain the "dromocrone" (Figure 5c). In the second step the 2D seismic wave velocity distribution on a section was determined using the Simultaneous Iterative Reconstruction Technique (SIRT) developed by Gilbert [23]. This inversion method is based on the least square principle [24]. The starting model corresponding to the homogeneous medium are compared with the measured data (travel times for each ray). This procedure is repeated with a continually changing model and the iterative process is halted when some stopping criteria are fulfilled, such as when

Table 1: Crown pillar probability failure definition over the long-term (from [20], modified).

class	Prob. of failure (%)	Minimum factor of safety	Serviceable Life	Years
A	50-100	<1	Effectively zero	0.5
B	20-50	1	Very very short term	1
C	10-20	1.2	Very short term	2-5
D	5-10	1.5	Short term	5-10
E	1.5 - 5	1.8	Medium term	15-20
F	0.5 - 1.5	2	Long term	50-100
G	<0.5	>>2	Very long term	>100

the root mean square of the residual travel times is smaller than a prefixed threshold.

Figure 6a illustrates the seismic wave velocity variation model. A low seismic velocity area is noted, labelled L ($500 < V_p < 700$ m/s).

Carrozzo et al. [25] used the Q system derived by [17] as the starting point for rockmass classification, and proposed a new approach with a modification of the Barton method for the classification of sedimentary rock mass (Q_{srm}). The study revises the correlation between V_p and Q derived by [17], deriving a new empirical equation correlating P -wave velocities and Q_{srm} values in soft sedimentary rock.

The modified relationship is [25]

$$V_p = V_0 k \log_{10} V_p = V_0 k \log_{10} (Q_{srm}/Q_0) \quad (5)$$

where V_0 is a P -wave velocity value characteristic of the subsoil volumes when $Q_{srm} = Q_0$. The factor k depends noticeably on the water content.

Using the relationship in (5), it is possible to obtain a model that shows variations in the Q_{srm} factor within the roof of the cave (Figure 6b). This model was used to estimate the Sc parameter (eq. (1)).

The next step was to study the stability of the roof using the empirical analysis described in the above paragraph. In the case of the model proposed by Hutchinson et al. [16] the crown pillar thickness (T) is considered to be constant. In our example the thickness varies with x , the distance along its length (Figure 7). Therefore $T = T(x)$, which takes into account the variations in thickness of the roof of the cave.

The variation of T as a function of the distance was modeled as a polynomial function

$$T(x) = 2E^{-7}x^6 - 2E^{-5}x^5 + 0.0009x^4 - 0.0185x^3 + 0.1864x^2 - 0.8057x + 2.1439 \quad (6)$$

Assuming $S.G. = 2.7$ and $\theta = 0$, the values of S and L were $S = 23$ m and $L = 2$ m.

Given these values and the seismic tomography results, the factor F (eq. (3)) was calculated using a code in matlab.

Results are shown in Figure 8, with the zone of instability ($F < 1$) marked as L .

4 3D seismic tomography survey

In order to obtain information about the instability areas present throughout the cave, a 3D seismic tomography survey was performed. At the studied site, the tomographic survey was designed with the fullest possible angular coverage. A rectangular area of 23×47 m located above the cave was selected (Figure 9); 144 receivers were arranged on the sides and in the central part of the study area. In particular, six acquisition lines were deployed: 3 lines in the NW – SE direction including 24 vertical, 14 Hz, 1 m spaced geophones; and 3 lines with 24 vertical 14 Hz geophones each oriented in the SSW – NNE direction and spaced at 2 m. 240 seismic source points were located as shown in Figure 9. All sources and receivers were located on the ground surface. A total of about 240 seismograms were made. The seismic source was a 5 kg hammer. Data were recorded on a 24 channel Geometrics strataview seismograph.

The seismic waves that travelling in the ground are recorded by the geophones laid on a ground surface. Both the seismic wave velocity and depth of the interfaces in the subsurface can be esteemed by measuring the seismic signal travel time between the sources and the receivers. In this paper the non-linear travel time tomography method was used. It consider the ray tracing for forward modeling and the simultaneous iterative reconstruction technique (SIRT) for inversion. In this case the velocity model is represented by quadrangle cells with dimensions that are chosen as the receiver interval (Figure 10).

By defined the ray as a line connecting the nodes arranged on the edges of the cell the first-arrival travel times (defined as the fastest travel time of all ray paths) and ray paths are calculated by the ray tracing method based on Huygen's principle [26]. Also in this case the starting model is updated by the SIRT (for more information see [27–29]).

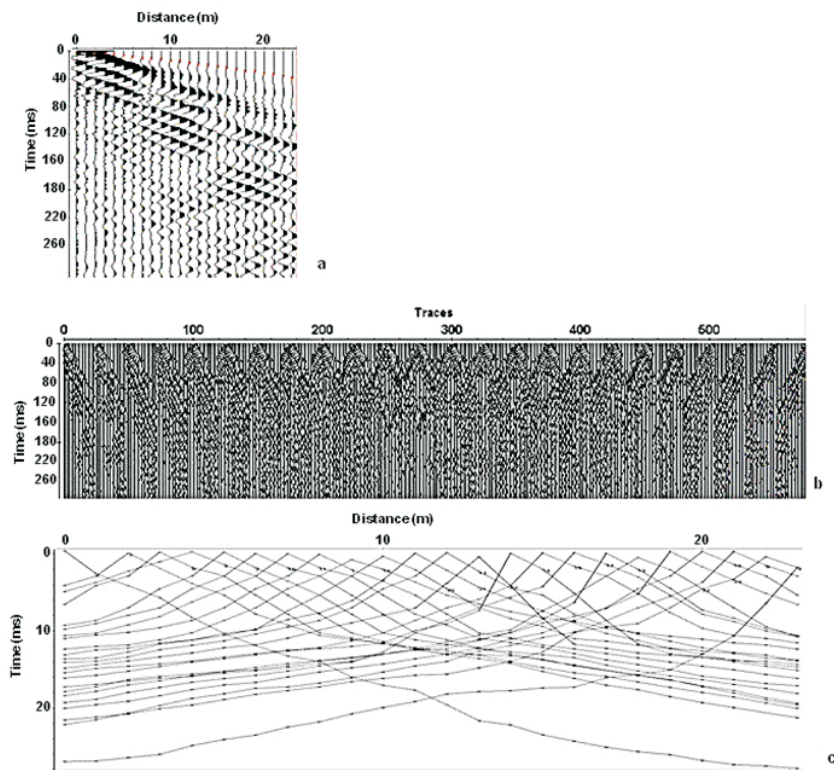


Figure 5: Seismic travel time tomography: a) an example of picking; b) the seismograms; c) dromochrones.

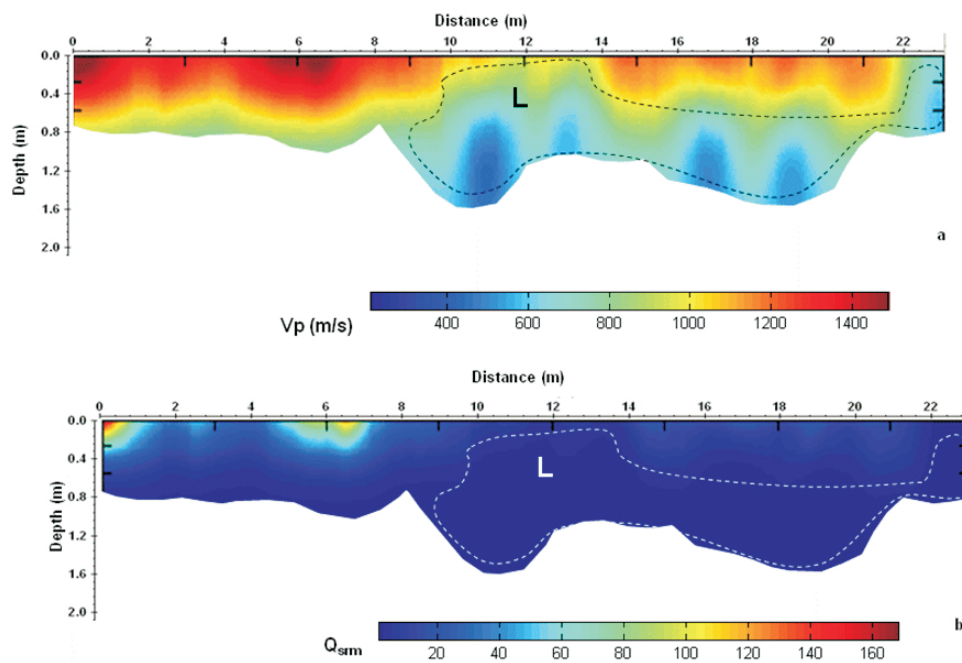


Figure 6: Seismic travel time tomography: a) V_p distribution; b) Q_{srm} distribution.

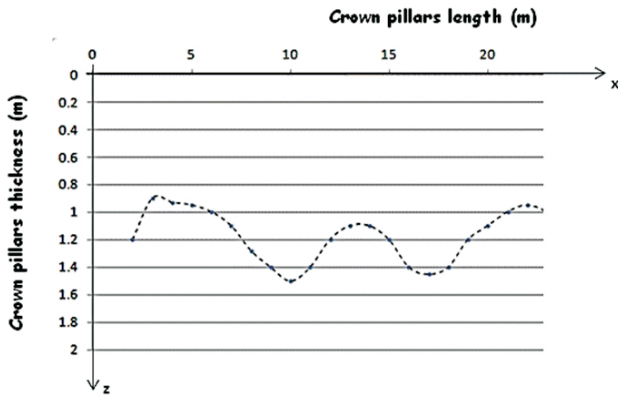


Figure 7: The crown pillar length as a function of crown pillar thickness.

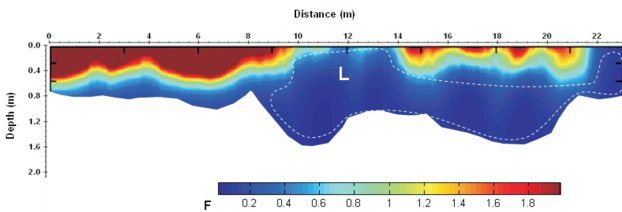


Figure 8: The F factor distribution.

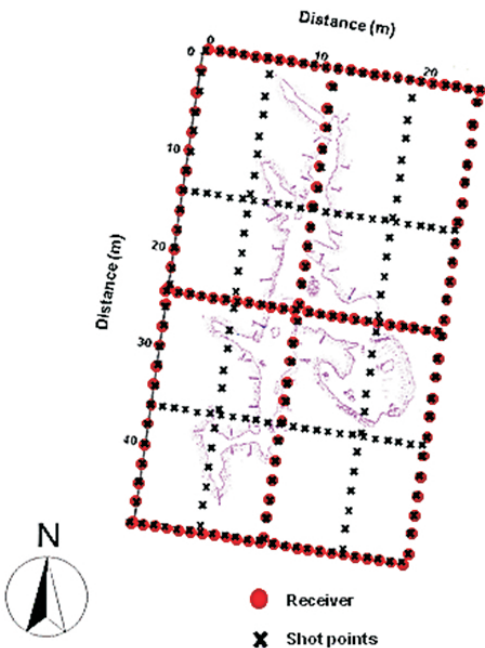


Figure 9: The acquisition geometry of the 3D seismic refraction tomography survey.

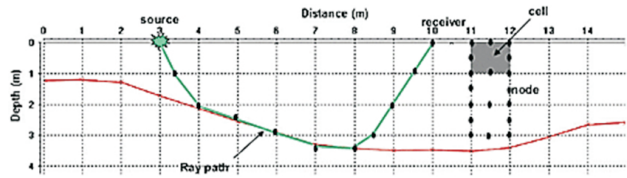


Figure 10: Principle of the ray tracing.

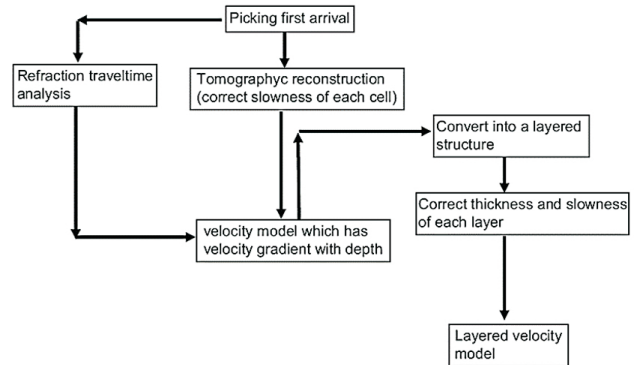


Figure 11: Processing flow for seismic refraction tomography data.

For seismic refraction tomography data processing and interpretation the software Reflexw 6.0, developed by Sandmeier [22] was used. The data processing flow is shown in Figure 11 [30].

The first step in the refraction tomography data processing was the travel times picking, consisting in the measure of first arrivals of seismic wave (Figure 12a). The first arrival travel times of each source and each receiver were combined in order to determine the velocity distribution on a 3D cube, (Figure 12b). Also in this case an homogeneous seismic velocity model was the initial velocity model used in the data inversion procedures.

The results of the inversion of seismic data are shown in Figure 13.

The 3D model generated by seismic refraction tomography, shown as depth slices, shows the variation of seismic P-wave velocity (V_p) in the subsurface. The seismic refraction tomography survey indicates that the shallow subsurface may be divided into two main zones. The first one (between 0 and 1 m depth), where V_p ranges from about 800 m/s to about 1800 m/s, corresponds to the location of the roof of the cave. The second one (1 to 1.75 m depth), characterized by the lowest seismic velocities (V_p ranging from about 200 m/s to about 400 m/s), corresponds to the location of the cave.

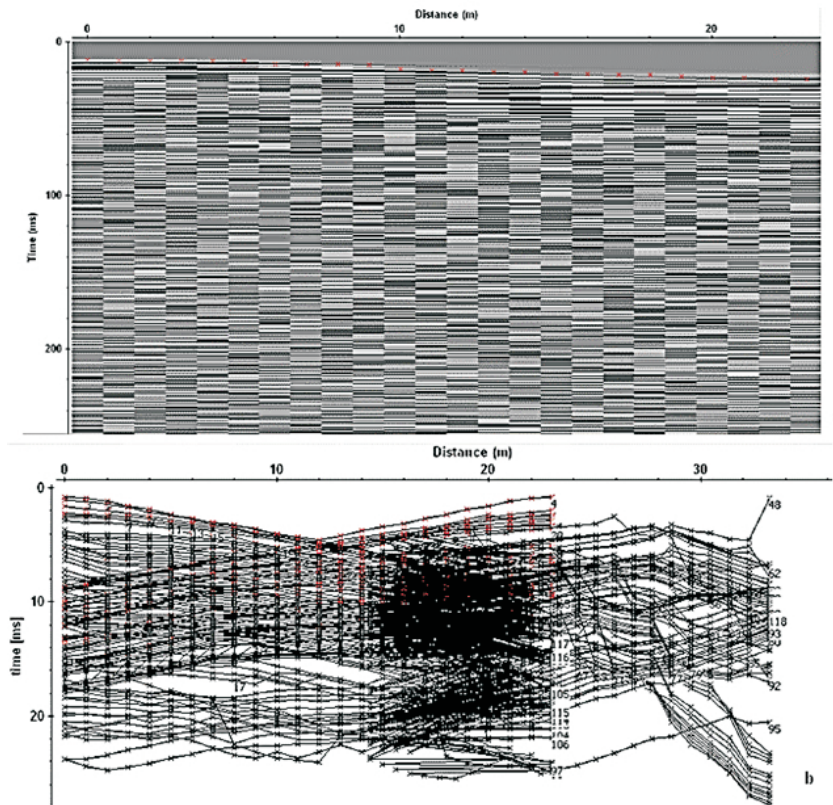


Figure 12: 3D Seismic refraction tomography: a) an example of picking; b) dromocrones.

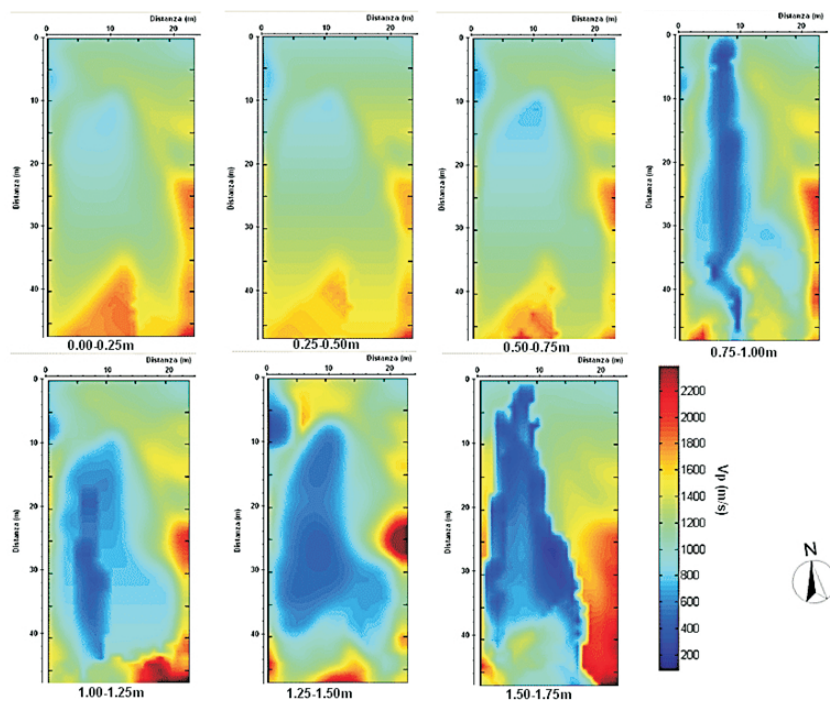


Figure 13: 3D Seismic refraction tomography: V_p depth slices.

3D images of seismic wave velocity were produced in order to better visualize the results (Figure 14). Seismic data were visualized as it follows:

- by a complete volume (Figure 14a); allowing the three-dimensional plotting of the data within pre-definable spatial limits (options x_{min}, \dots, z_{max}) and an arbitrarily definable observation point ($\mathbf{x}^\circ, \mathbf{y}^\circ$ and \mathbf{z}°);
- by single sections (Figure 14b); allowing any combination of x -, y - or z -cross-sections to be plotted. This visualization makes it easier to determine the thickness of the roof of the cave;
- by 3D contouring of iso-velocity surfaces (Figure 14c). In this representation the transparency function is defined by two threshold values of the velocity, V_{p1} and V_{p2} ($V_{p1} < V_{p2}$). In the intervals $V_p < V_{p1}$ and $V_p > V_{p2}$, data are rendered as transparent, therefore only the data in the interval $V_{p1} < V_p < V_{p2}$ are visualized. In Figure 14c the seismic data set is displayed with iso-velocity surfaces using a threshold value ranging from 200 to 500 m/s. This V_p threshold value makes the possible location of the cave more obvious.

The next step was to study the stability of the roof using the empirical analysis described in the previous paragraph. In this case the thickness, T , varies with the distance x and y because it takes into account the variations in thickness of the roof of the cave. Therefore T is treated as a matrix.

Consider a parametric surface parameterized by two independent variables, i and j , which vary continuously over a rectangle; for example, $1 \leq i \leq m$ and $1 \leq j \leq n$. Matrix T was constructed considering the measured distance x , y and the thickness z calculated from the results of the 3D seismic data.

Using equations (1-3), the factor of safety F was calculated using a 3D matlab code from the seismic tomography results. It was assumed that $S.G. = 2.7$, $\theta = 0$ (i.e. waste rock that is not dipping). Values of S and L were derived from geophysical measurements and held constant ($S = 47$ m, $L = 13$ m). The resulting zones of instability ($F < 1$) in the surveyed area were identified and can be seen in Figure 15. In Figure 16 the zones representing the distribution of the F factor at 0.25-0.50 m and 0.75-1.0 m depth are superimposed on the plan of the cave. It shows several zones of instability ($F < 1$).

5 Conclusions

Non-destructive geophysical prospecting techniques play a strategic role in the resolution of many issues relating to the conservation and protection of cultural and environmental heritage. Numerous methods of investigation can be used (electrical methods, seismic methods, electromagnetic methods, etc ...). When these are integrated with observations and results from other disciplines such as geology, geomorphology, physics and/or engineering, we can obtain a range of information about the site being studied. In this paper the potential of seismic methods for studying the stability conditions of a cave of archaeological importance were assessed. Seismic data were used as the starting point for applying empirical analysis imported from mining engineering: the "scaled span" method.

The combined use of 2D seismic travel time tomography and 3D seismic tomography has made it possible to obtain 2D and 3D distributions of P -wave velocity propagation in the rock forming the ceiling of a cave.

In the 2D seismic wave velocity model an area in which the V_p is relatively low ($500 < V_p < 700$ m/s) is clearly visible. In other areas the values of V_p are between 1100 m/s and 1500 m/s. By correlating the values of P -wave velocity with the Q_{rsm} value that describes the quality of the rock, it is clear that the low-velocity area corresponds to an area of the cave in which the calcarenite-type rock is of low quality.

From the 3D seismic wave velocity model, the 3D dimensions of the cave and the 3D dimensions of the thickness of the ceiling of the cave are clearly visible. It is noted also that the zone between 0 and 1 m depth has seismic wave velocities (V_p) ranging from about 800 m/s to about 1800 m/s, corresponding to the area in which the roof of the cave is located. In this area the low V_p zones are also related to the low quality of the calcarenite rock. After determining the Q_{rsm} parameter of the rock mass quality, the analysis of the stability of the vault of the karst cave was performed in 2D and 3D.

In this paper the empirical analysis proposed by Hutchinson [16] was adapted to the geometry of a karstic cave. The study of stability was performed considering the crown pillar thickness as a variable function of the length x in the 2D case and as a function of the length x and width y in the 3D case.

The model indicates instability when the coefficient C_s is larger than critical amplitude S_c , evaluated according to the terms described in the paper. From the ratio S_c/C_s , denoted by the failure of safety factor F , it is possible to con-

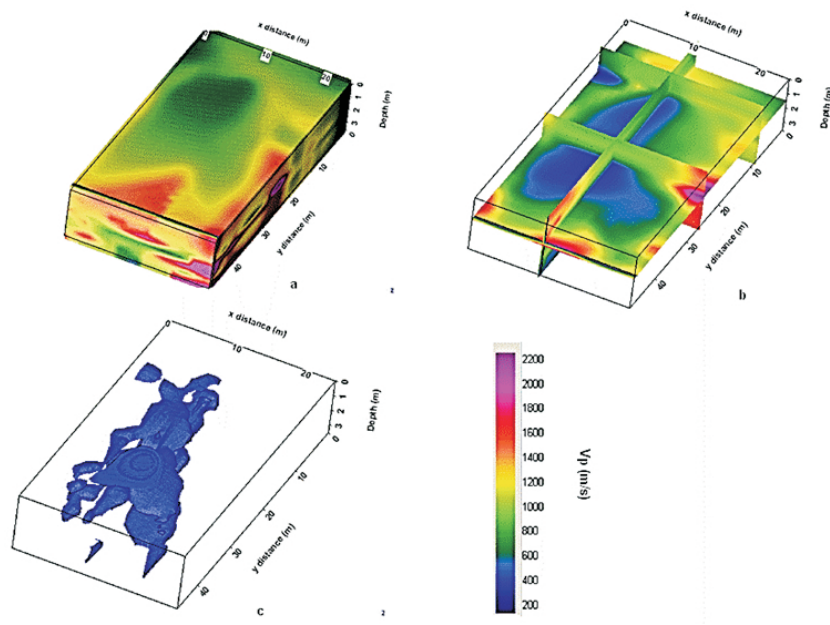


Figure 14: 3D Seismic refraction tomography; 3D visualization: a) complete volume; b) single sections; c) 3D contouring of iso – velocity surfaces.

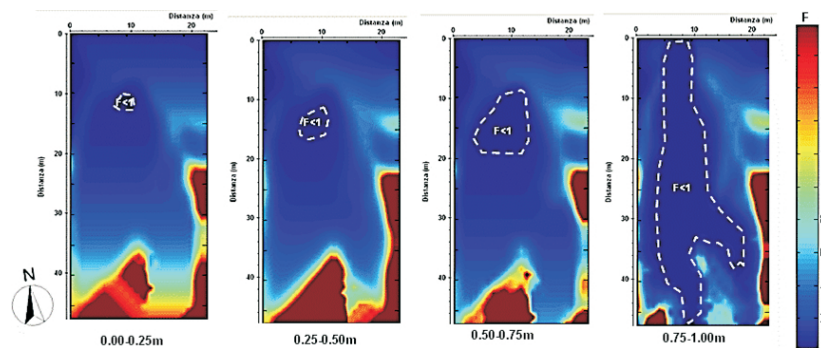


Figure 15: 3D Seismic refraction tomography: F factor depth slices.

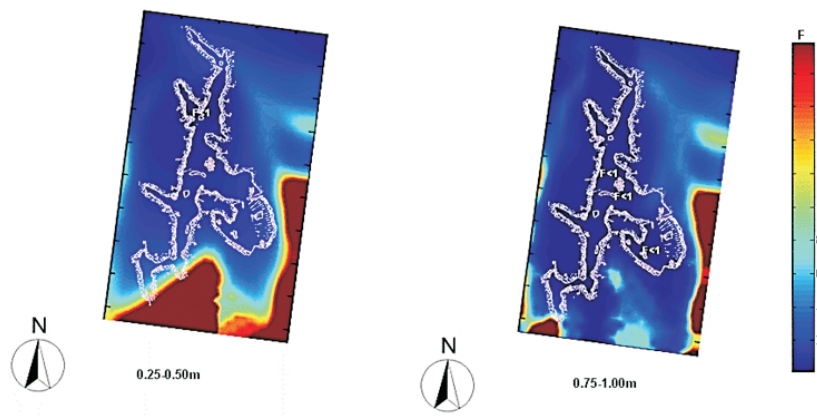


Figure 16: The models representing the distribution of the F factor at 0.25-0.50m and 0.75-1.0m in depth superimposed on the plan of the cave.

clude that where F is less than 1 the rock formation is dominantly unstable.

For this study a 2D and a 3D distribution of the F factor were calculated. In the 2D case the region of greater instability of the cave corresponds with the area marked "L" (Figure 8). In the 3D case there are several zones with $F < 1$ (Figure 15, Fig 16).

Using Table 1 it is possible to deduce that in the zones with $F < 1$, the probability of rock failure is in the range between 50 and 100%. According to Table 1, the rock failure could happen in about 0.5 years.

This study highlights how seismic investigations are of fundamental importance in an area where it is not possible to apply direct methods. Seismic tomography was crucial in studying the physical – mechanical properties of the rock. Furthermore, the results obtained were used as inputs in the application of the empirical analysis of stability proposed by Hutchinson (adapted to natural underground cavities). Thus, a synergic use of seismic techniques and analytical models can be recommended for the study of any site in which a karstic hazard is a risk. From this type of study it is possible to obtain information indicative of the degree of stability to help with preserving the safety of people and cultural heritage.

References

- [1] Cremonesi G., La passione per l'origine, Giliano Cremonesi e la passione preistorica nel salento, 1987, 213–245.
- [2] Leucci G., De Giorgi L., Integrated geophysical surveys to assess the structural conditions of a karstic cave of archaeological importance, *Natural Hazards and Earth System Sciences*, 5, 2005, 17-22.
- [3] Catani F., Fanti R., Moreti S., Geomorphologic risk assessment for cultural heritage conservation, in: Allison R.J. (Ed.), *Applied Geomorphology: theory and practice*, John Wiley & Sons, LTD, West Sussex, England, 2002, 480.
- [4] Sánchez M. A., Foyo A., Tomillo C., Iriarte E., Geological risk assessment of the area surrounding Altamira Cave: A proposed Natural Risk Index and Safety Factor for protection of prehistoric caves *Engineering Geology* 94, 2007, 180–200.
- [5] Veni G., A geomorphological strategy for conducting environmental impact assessments in karst areas, *Geomorphology* 31, 1999, 151-180.
- [6] Lin Z., Hatherly P., Vozoff K., Engels O. G., Smith G. H., Joint application of seismic and electromagnetic methods to coal characterisation at west cliff colliery, New South Wales, *Experiment in Geophysics* 27(4), 1996, 205–215.
- [7] Dobroka M., Gyulai A., Ormos T., Csokas J., Dresen L., 1991. Joint inversion algorithm of seismic and geoelectric data recorded in an underground coal mine. *Geophysical Prospecting* 39(5), 1991, 643–666.
- [8] Heikkinen E.J., Saksa P.J., Integrating geophysical data into bedrock model in site characterization for nuclear waste disposal. 60th Mtg. Eur. Assoc. Expl Geophys., Expanded Abstracts, vol. I. EAGE, The Netherlands, 1998, Session 4–49.
- [9] Santarato G., Nasser A., Chiara P., *Prospezioni geofisiche in area urbana*, *Geologia Tecnica e Ambiente* 4/98, 1998, 43–52.
- [10] Cardarelli E., Marrone C., Orlando L., Evaluation of tunnel stability using integrated geophysical methods, *Journal of Applied Geophysics* 52, 2003, 93–102.
- [11] Leucci G., De Giorgi L., Microgravimetric and ground penetrating radar geophysical methods to map the shallow karstic cavities network in a coastal area (marina di capilungo, lecce –italy), *Exploration Geophysics* 41, 2010, 178-188.
- [12] Crampin S., McGonigle R., Bamford D., Estimate crack parameters from observation of P-wave velocity anisotropy, *Geophysics* 45, 1980, 361–375.
- [13] Boadu F. K., Fractured rock mass characterization parameters and seismic properties: analytical studies, *J. Appl. Geophys.* 36, 1997, 1–19.
- [14] Kahraman S., The effects of fracture roughness on P-wave velocity, *Eng. Geol.* 63, 2002, 347–350.
- [15] Leucci G. and De Giorgi L., Experimental studies on the effects of fracture on the P and S wave velocity propagation in sedimentary rock ("Calcarenite del Salento"), *Engineering Geology* 84, 2006, 130–142.
- [16] Hutchinson D. J., Phillips C. and Cascante G., Risk considerations for crown pillar stability assessment for mine closure planning, *Geotechnical and Geological Engineering* 20, 2002, 41-63.
- [17] Barton N., Some new Q-value correlations to assist in site characterisation and tunnel design, *Int. J. Rock Mech. Min. Sci.* 39, 2002, 185-216.
- [18] Carter T. G., A new approach to surface crown pillar design. 16th Canadian Rock Mechanics Symp., Laurentian University, Sudbury, 1992, 75-84.
- [19] Barton N., Lien R. and Lunde J., Engineering classification of rockmasses for the design of tunnel support, *Rock Mech.* 6(4), 1974, 189-236.
- [20] Carter T. G. and Miller R. I., Crown pillar risk assessment planning aid for cost-effective mine closure remediation, *Trans. Instn. Min. Metall.* 104, 1995, A41-A57.
- [21] Leucci G., I metodi elettromagnetico impulsivo, elettrico e sismico tomografico a rifrazione per la risoluzione di problematiche ambientali: sviluppi metodologici e applicazioni, PhD tesi in Geophysics for Environmental and Territory, University of Messina, 2004.
- [22] Sandmeier K. J., *Reflexw 6.0 Manual*, Sandmeier Software, Zipser Strabe 1, D-76227 Karlsruhe, Germany, 2011.
- [23] Gilbert P., Iterative methods for three-dimensional reconstruction of an object from projections, *Journal of Theoretical Biology* 36, 1972, 105-117.
- [24] Krajewski C., Dresen L., Gelbke C., Ruter H., Iterative tomographic methods to locate low-velocity anomalies: a model study, *Geophysical Prospecting* 37, 1989, 717-751.
- [25] Carrozzo M. T., Leucci G., Margiotta S., Mazzone F., Negri S., Integrated geophysical and geological investigations applied to sedimentary rock mass characterization *Annals of Geophysics* 51(1), 2008, 191-202.
- [26] Parasnis D. S., *Principles of Applied Geophysics*, fifth ed., Chapman and Hall, London, 1997.

- [27] Hayashi K., Takahashi T., High resolution seismic refraction method using surface and borehole data for site characterization of rocks, *International Journal of Rock Mechanics and Mining Sciences* 38, 2001, 807-813.
- [28] Morey D., Schuster G. T., Paleoseismicity of the Oquirrh fault, Utah from shallow seismic tomography, *Geophysical Journal International* 138, 1999, 25-35.
- [29] Nemeth T., Normark E., Qin F., Dynamic smoothing in cross-well travelttime tomography, *Geophysics* 62, 1997, 168-176.
- [30] Leucci G., Greco F., De Giorgi L., Mauceri R., Three-dimensional image of seismic refraction tomography and electrical resistivity tomography survey in the castle of Occhiolà (Sicily, Italy), *Journal of Archaeological Science* 34, 2007, 233-242.